



SPIO

:

1

2

3

Superparamagnetic iron oxide (, SPIO)
 가
 : 가 SPIO 68
 , 4 ; 가 10
 (9 , 1), Child's A 25 (22), Child's B 15 (11
), Child's C 18 (10). SPIO , T2 -
 , T2 -
 , SPIO ,
 , SPIO
 : SPIO T2 - T2 -
 T2 -
 ,
 (p < 0.05).
 Child's B Child's
 (p < 0.0001), SPIO
 (p > 0.05).
 C Child's A
 ,
 (p < 0.05).
 : SPIO Child's
 , SPIO Child's B Child's C

Superparamagnetic iron oxide (, SPIO) 가
 Kupffer
 (reticuloendothelial system) , T2 가 (7, 8). ,
 SPIO 가 (8-13),
 가 (1-4). SPIO (8, 9).
 Kupffer (hepato - SPIO
 Kupffer (5, 6).
 cyte) , SPIO
 , SPIO
 가

1
 2
 3
 2000 3 8 2000 7 18

: SPIO

Table 1. Summary of Clinical Data in Patients Performed SPIO-Enhanced MRI

	Normal (n = 10)	Child's A (n = 25)	Child's B (n = 15)	Child's C (n = 18)
Mean Age (years)	50.2	62.7	57	47
M/F	7/3	22/3	13/2	14/4
Final Diagnosis				
Hemangioma	9	0	0	0
Hepatic cyst	1	0	0	0
HCC*	0	22	11	10
Regenerative nodule	0	3	4	8

*HCC = hepatocellular carcinoma

가 SPIO
68
4 = 10
Child's A = 25, Child's B = 15,
Child's C = 18
Table 1 10 9

58 CT
가 가 SPIO
43 51
28
15 가 (> 400 ng/ml),
(tumor staining) CT
0.8 - 6.5 cm (, 3.6 cm)

1.5T (Magne-
tom Vision; Siemens, Erlangen, Germany)
(phased array multi-coil) SPIO
T2- (conventional T2-
weighted spin echo, conventional T2-weighted SE)
(TR/TE = 2900 - 3500 msec/90 msec, one signal acquired,
a 104 - 192 x 256 matrix), T2-
(respiratory-triggered T2-weighted turbo spin echo,

RT T2-weighted TSE) (TR/TE/echo train lengths =
2,100 - 4500 msec/90 msec/5, two signals acquired, a 100 -
192 x 256 matrix), T2-
(breathhold T2-weighted turbo spin echo, BH T2-
weighted TSE) (TR/TE/echo train lengths = 2900 - 3100
msec/138 msec/29, one signal acquired, a 116 x 256 matrix)
24

SPIO
SPIO 100 ml 5% 10
µmol/kg SPIO (Feridex; Advanced Magnetics,
Cambridge, U.S.A.) 30
10 2 ml
4 ml SPIO 1
4 SPIO
, 1 가

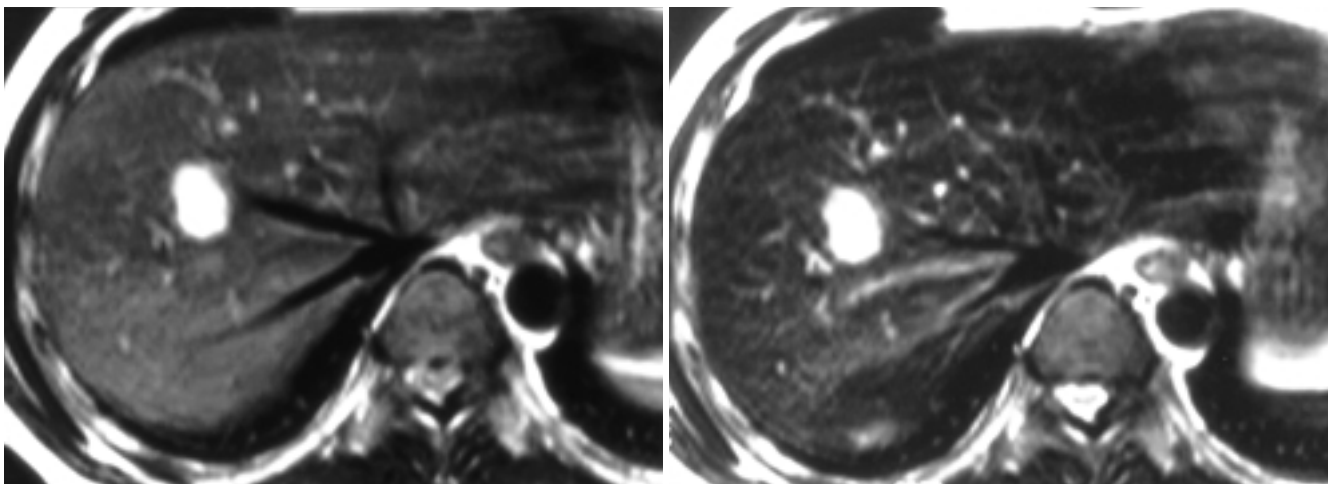


Fig. 1. A, B. Conventional T2-weighted turbo spin echo images before (A) and after (B) administration of SPIO in a 46-year-old man with hemangioma in right lobe of liver. The percentage of signal intensity loss of hepatic parenchyma after administration of SPIO is 69.7% in normal liver.

SPIO (region of interest, ROI) 가 가 ROI SPIO (albumin), (alanine aminotrasferase, ALT), (aspartate aminotransferase, AST), (prothrombin time, PT) SPIO (correlation coefficient) p 0.05

(phase encoding direction) SPIO (percentage of signal intensity loss) Percentage of signal intensity loss = [() / ()] x 100.

Child's one-way Anova Test , p 0.05 가

SPIO ; 1 - , 2 - , 3 가 가(unacceptable, 1), (poor, 2), (fair, 3), (good, 4) (excellent, 5) 5 가 SPIO RT T2-weighted TSE Wilcoxon signed ranks test SPIO conventional T2-weighted SE가 50.9±21.2 , RT T2-weighted TSE BH T2-weighted TSE 44.1±19.1, 39.6±17.4 (p < 0.05), Child's C (p < 0.05) (Table 2) (Fig. 1, 2). Table 3

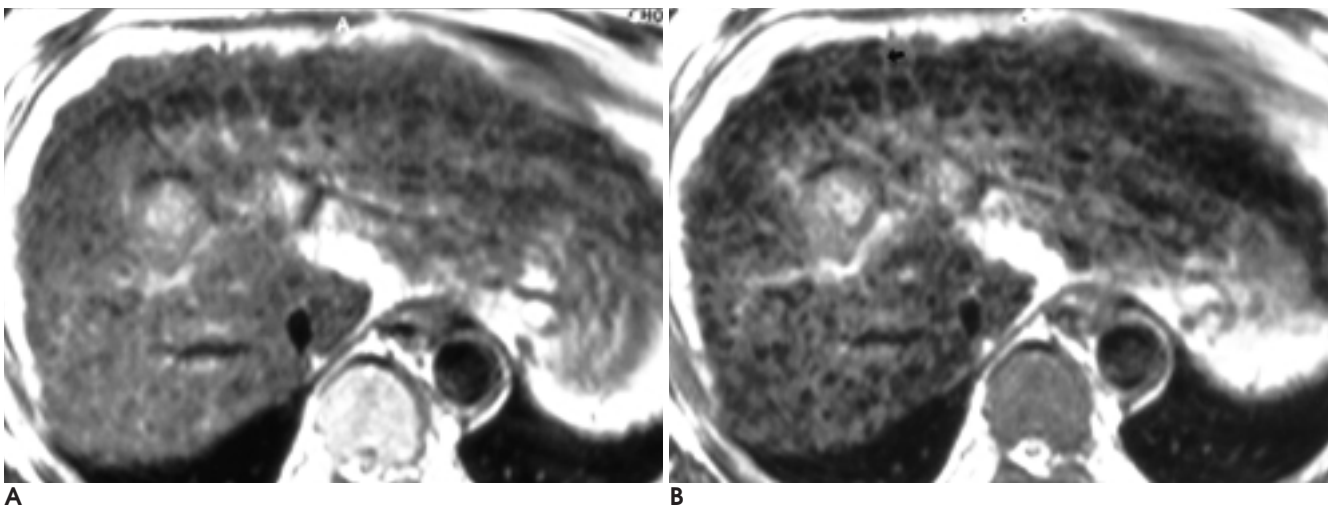


Fig. 2. A, B. Conventional T2-weighted turbo spin echo images before (A) and after (B) administration of SPIO in a 36-year-old man with severe degree of liver cirrhosis (Child's class C). The percentage of signal intensity loss of hepatic parenchyma after administration of SPIO is 17.6% (cirrhotic liver). Inhomogeneous appearances of hepatic parenchyma by fibrous septa (arrow) are seen after administration of SPIO (B).

: SPIO

Child's B C
 Child's A
 ($p < 0.0001$) (Fig. 3).
 Child's A B SPIO
 가 ($p < 0.05$), Child's
 C 가 ($p = 0.39$) (Table
 4). SPIO Child's C
 ($p > 0.05$). Child's C 1
 (Fig. 4).

PT (Table 5).
 - MR SPIO
 Kupffer (reticuloendothelial
 system) T2
 가 T2
 가 가 (1-3). SPIO
 가 ,

SPIO
 conventional T2-weighted SE BH T2-weighted TSE
 , , PT
 , RT T2-weighted TSE , ALT,

Table 2. Percentage of Signal Intensity Loss of the Liver of Conventional T2-Weighted SE Imaging, Respiratory-triggered T2-Weighted TSE Imaging and Breathhold T2-Weighted TSE Imaging

	Conventional T2wSE	BT-T2wTSE	BH-T2wTSE
Normal (n=9)	64.2 ± 19.3	61.1 ± 14.3	45.3 ± 25.6
Child's class A (n=19)	55.9 ± 12.4	42.1 ± 17.8	43.1 ± 12.4
Child's class B (n=8)	51.3 ± 17.5	36.3 ± 23.6	36.7 ± 16.5
Child's class C (n=8)	14.8 ± 6.1	31.6 ± 7.8	22.4 ± 3.4
P-value	< 0.0001	0.008	0.044

Note - Values are expressed as mean ± SD.
 T2wSE = T2-Weighted spin echo,
 BT-T2wTSE = breath-triggered T2-Weighted turbo spin echo,
 BH-T2wTSE = breathhold T2-Weighted turbo spin echo.

Table 3. Results of Qualitative Analysis of MR Appearance of the liver after SPIO-Enhancement

MR Appearance of the Liver	
Normal (n = 10)	1.00
Child's A (n = 25)	1.28 ± 0.55
Child's B (n = 15)	2.31 ± 0.69*
Child's C (n = 18)	2.56 ± 0.59*
Mean (n = 68)	1.94 ± 0.63

Note - Values are expressed as mean ± SD.
 * - significant difference with Child's A ($p < 0.0001$)

Table 4. Results of Qualitative Analysis of Lesion Conspicuity before and after SPIO-enhancement

	Before SPIO-enhancement	After SPIO-enhancement
Child's A (n = 22)	3.00 ± 1.19	4.38 ± 0.8*
Child's B (n = 11)	3.10 ± 0.92	3.97 ± 0.74*
Child's C (n = 10)	3.12 ± 1.34	3.69 ± 1.6
Mean (n = 43)	3.23 ± 1.14	4.37 ± 1.28*

Note - Values are expressed as mean ± SD.
 * - significant difference with before SPIO-enhancement ($p < 0.05$)

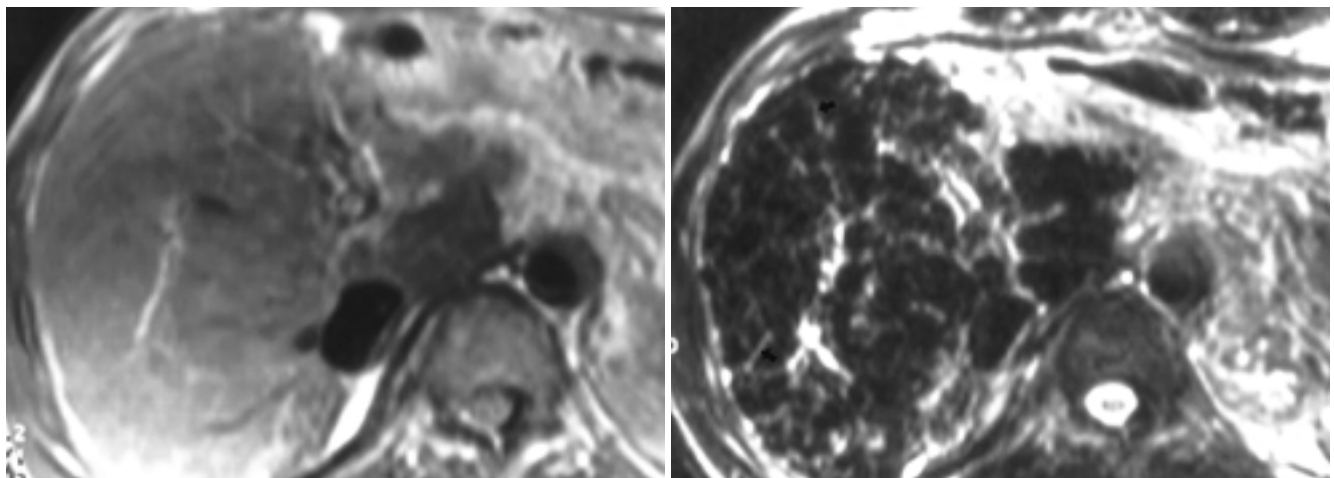


Fig. 3. A, B. Conventional T2-weighted turbo spin echo images before (A) and after (B) administration of SPIO in 44-year-old man with severe degree of liver cirrhosis (Child's class C). Inhomogeneous appearances of hepatic parenchyma by fibrous septa (arrows) are seen after administration of SPIO (B).

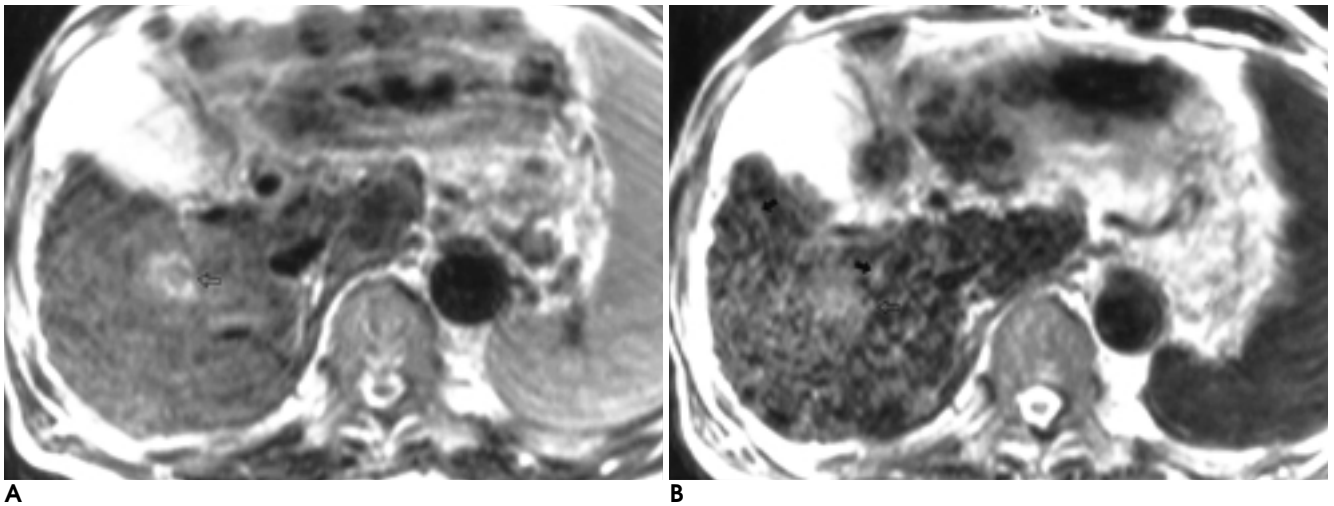


Fig. 4. 61-year-old man with severe liver cirrhosis (Child's class C) and hepatocellular carcinoma. SPIO-enhanced respiratory-triggered turbo-spin echo image (B) shows lower lesion conspicuity (open arrow) than SPIO-unenhanced image (A) due to inhomogeneous appearances of hepatic parenchyma by fibrous septa (arrows) and multiple nodules with low signal intensity in severe cirrhotic liver.

Table 5. Relationship between Percentage of Signal Intensity Loss of Liver and Liver Function Test

Liver Function Test	Correlation Coefficient		
	Conventional T2wSE	BT-T2wTSE	BH-T2wTSE
Albumin	0.455**	0.456**	0.326*
Total bilirubin	-0.571**	-0.261	-0.370*
ALT	-0.206	-0.353*	-0.127
AST	0.055	-0.129	-0.013
PT	0.585**	0.512**	0.468**

Note - Values are expressed as correlation coefficient.

T2wSE = T2-Weighted spin echo,

BT-T2wTSE = breath-triggered T2-Weighted turbo spin echo,

BH-T2wTSE = breathhold T2-Weighted turbo spin echo,

PT = prothrombin time.

* : Correlation is significant at the 0.05 level.

** : Correlation is significant at the 0.01 level

(2, 4, 7, 14 - 15).
SPIO 가
(8 - 13),

Yamashita (9) SPIO
가 ,
가 ,
SPIO
Child's C

SPIO T2 -
. , SPIO

T2* -

가 (1).
TSE conventional SE
(16). TSE rephras -
ing pulse (magnetic susceptibility)
T2* - 가
, conventional SE가
(17). , T2* -
가
(17). RT T2 -
weighted TSE conventional SE가 가
가 (imaging artifact)
가 가 RT T2 -
weighted TSE
SPIO 80 - 160 nm, 8
80%가 Kupffer cell
6%가 ,
(18). (scintigraphy)
sulfur colloid가
Kupffer
sulfur colloid 가
가 가 (5 - 6), SPIO
가 가
가
SPIO 가 , 3가

: SPIO

(intrahepatic shunt)
(portosystemic shunt)

가 Kupffer 가 . ,
가
(opsonin) Kupffer
가 (5, 11), 가
SPIO Kupffer 가
Kupffer
(5, 19), SPIO
Yamashita (9) SPIO
AST 가
SPIO PT
ALT Kupffer
SPIO 가 가
가 (9, 11).
SPIO
Kupffer
SPIO
Child's B C
SPIO
가
SPIO
Child's A (8). SPIO Child's C
SPIO
Child's C 1
s C

Child's (9)
Yamashita SPIO
Kupffer 가
Kupffer
Child's SPIO
가
SPIO 가
SPIO
Child's
Albumin, PT
SPIO
Child's C SPIO
가 SPIO

1. Fetz CJ, Elizondo G, Weissleder R, et al. Superparamagnetic iron oxide-enhanced MR imaging: pulse sequence optimization for detection of liver cancer. *Radiology* 1989;172:393-397
2. Tsang YM, Stark DD, Chen MC, Weissleder R, Wittenberg J, Ferrucci JT. Hepatic micrometastasis in the rat: ferrite-enhanced MR imaging. *Radiology* 1988;167:21-24
3. Saini S, Stark DD, Hahn PF, et al. Ferrite particles: a superparamagnetic MR contrast agent for enhanced detection of liver carcinoma. *Radiology* 1987;162:217-222
4. Stark DD, Weissleder R, Elizondo G, et al. Superparamagnetic iron oxide: clinical application as a contrast agent for MR imaging of the liver. *Radiology* 1988;168:297-301
5. Imawari M, Hughes RD, Gove CD. Fibronectin and Kupffer cell function in fulminant hepatic failure. *Dig Dis Sci* 1985;30:1028-1033
6. Kim E, Domstad P, Chov Y, Coupal J, DeLand F. Complementary role of reticuloendothelial and hepatobiliary imaging agents in the assessment of liver disease. *Clin Nucl Med* 1982;7:64-66
7. Yamamoto H, Yamashita Y, Yoshimatsu S, et al. Hepatocellular carcinoma in cirrhotic liver: detection with unenhanced and iron oxide-enhanced MR imaging. *Radiology* 1995;195:106-112
8. Tang Y, Yamashita Y, Arakawa A, et al. Detection of hepatocellular carcinoma arising in cirrhotic livers: comparison of gadolinium- and ferumoxides-enhanced MR imaging. *AJR Am J Roentgenol* 1999; 172:1547-15545
9. Yamashita Y, Yamamoto H, Hirai A, Yoshimatsu S, Baba Y, Takahashi M. MR imaging enhancement with superparamagnetic iron oxide in chronic liver disease: influence of liver dysfunction and parenchymal pathology. *Abdom Imaging* 1996;21:318-323
10. Kreft B, Block W, Dombrowski F, et al. Diagnostic value of a superparamagnetic iron oxide in MR imaging of chronic liver disease in an animal model. *AJR Am J Roentgenol* 1998;170:661-668
11. Elizondo G, Weissleder R, Stark DD, et al. Hepatic cirrhosis and

- hepatitis: MR imaging enhanced with superparamagnetic iron oxide. *Radiology* 1990;174:797-801
12. Reimer P, Weissleder R, Lee AS, et al. Asialoglycoprotein receptor function in benign liver disease: evaluation with MR imaging. *Radiology* 1991;78:769-774
 13. Clement O, Frija G, Chambon C, et al. Liver tumors in cirrhosis: experimental study with SPIO-enhanced MR imaging. *Radiology* 1991;180:31-36
 14. Fretz CJ, Stark DD, Metz CE, et al. Detection of hepatic metastasis: comparison of contrast-enhanced CT, unenhanced MR imaging, and iron-oxide-enhanced MR imaging. *AJR Am J Roentgenol* 1990;155:763-770
 15. Seneterre E, Taourel P, Bouvier Y, et al. Detection of hepatic metastasis: ferumoxides-enhanced MR imaging versus unenhanced MR imaging and CT during arterial portography. *Radiology* 1996;200:785-792
 16. Schwartz LH, Seltzer SE, Tempany CMC, et al. Superparamagnetic iron oxide hepatic MR imaging: efficacy and safety using conventional and fast spin-echo pulse sequences. *J Magn Reson Imaging* 1995;5:566-570
 17. , , , et al. : SPIO : Gd-DTPA . 2000;42:265-272
 18. Weissleder R, Hahn PF, et al. Superparamagnetic iron oxide: enhanced detection of splenic tumors with MR imaging. *Radiology* 1988;169:399-403
 19. Milward-Sadler G, Wright R. *Cirrhosis: an appraisal*. In: Wright R, Albert K, Karran S, et al, eds. *Liver and biliary disease*. Philadelphia: Saunders, 1979;688-714

Superparamagnetic Iron Oxide Enhanced MR Imaging: Influence of Hepatic Dysfunction in Cirrhotic Patients¹

Hyo-Sung Kwak, M.D., Jeong-Min Lee, M.D., Seong-Hee Ym, M.D.², Chong-Soo Kim, M.D.,
Hyun-Young Han, M.D.³

¹Department of Diagnostic Radiology, Chonbuk National University Hospital

²Department of Internal Medicine, Namwon Medical Center

³Department of Diagnostic Radiology, Eulgy University Hospital

Purpose: To determine the influence of liver dysfunction on the detection of focal hepatic nodules, and to investigate the loss of signal intensity of hepatic parenchyma occurring after superparamagnetic iron oxide (SPIO)-induced contrast enhancement in patients with liver cirrhosis.

Materials and Methods: In 68 patients with liver cirrhosis, we evaluated MR images before and after the administration of SPIO. Clinical information and laboratory data indicated that the liver was normal in ten patients (nine hemangiomas and one hepatic cyst), while Child's A was diagnosed in 25 cases [22 of which were hepatocellular carcinomas (HCCs)], Child's B in 15 (11 HCCs), and Child's C in 18 (10 HCCs). Before and after SPIO administration, conventional T2-weighted spin-echo, respiratory-triggered T2-weighted turbo spin-echo, and breathhold T2-weighted turbo spin-echo images were obtained. After the administration of SPIO, degrees of liver dysfunction and laboratory data were correlated with reductions in signal intensity of the liver, and, in addition, the state of hepatic dysfunction was correlated with inhomogeneous parenchymal change and lesion conspicuity.

Results: After the administration of SPIO, percentage signal loss in liver parenchyma was significantly higher on conventional T2-weighted spin-echo images than on T2-weighted turbo spin-echo and breathhold T2-weighted turbo spin-echo ($p < 0.05$). There was significant correlation between degree of liver dysfunction and of signal loss ($p < 0.05$), while percentage signal loss of the liver was lower in the Child's C group than in the other three. In addition, there was close correlation between percentage signal loss and laboratory data such as albumin and total bilirubin levels, and prothrombin time ($p < 0.05$). Qualitative analysis showed that inhomogeneous enhancement due to fibrous septa and a regenerative nodule occurred more often in the Child's B and Child's C group than in the normal and Child's A group ($p < 0.0001$). In terms of lesion conspicuity, there was no statistically significant difference between the groups ($p > 0.05$).

Conclusion: SPIO uptake by hepatic parenchyma correlated closely with Child's degree of liver cirrhosis and laboratory data such as albumin and total bilirubin levels, and prothrombin time. In the Child's B and Child's C group, SPIO-enhanced MR imaging revealed inhomogeneous hepatic parenchyma, but the pattern observed did not affect the detection of hepatic nodules.

Index words : Superparamagnetic iron oxide, MR imaging
Contrast agent, liver cirrhosis
Magnetic resonance (MR), contrast media

Address reprint requests to : Jeong-Min Lee, M.D., Department of Diagnostic Radiology, Chonbuk National University Medical School
634-18 Keumam-Dong, Chonju-shi, Chon Buk 561-712, Korea.
Tel. 82-63-250-1172 Fax. 82-63-272-0481